Steel and Composite Structures, Vol. 11, No. 5 (2011) 359-374
DOI: http://dx.doi.org/10.12989/scs.2011.11.5.359

Influence of aspect ratio and fibre orientation on the stability of simply supported orthotropic skew plates

Kutlu Darilmaz*

Department of Civil Engineering, Istanbul Technical University 34469, Maslak, Istanbul, Turkey

(Received March 13, 2011, Revised May 02, 2011, Accepted June 10, 2011)

Abstract. In this paper, the influence of fibre orientation and aspect ratio on stability analysis of simply supported skew plates subjected to in plane loading is studied by using a four noded hybrid plate finite element. The formulation of the element is based on Hellinger-Reissner variational principle. The element is developed by combining a hybrid plane stress element and a hybrid plate element. Some numerical problems are solved and the effects of skew angle, aspect ratio, fibre orientation and loading type on the critical buckling loads are highlighted.

Keywords: stability; buckling; orthotropic plate; fibre orientation; boundary condition; hybrid finite element

1. Introduction

Skew plates are widely used in modern structures as structural elements of practical importance. With the wide use of fibrous plate structures in modern industries, stability analysis of skew plates of different geometry becomes an important design procedure. An adequate understanding of the stability of these plate components, is important to the design and performance evaluation of a system. However, such solutions to these plate problems are strongly dependent on the geometrical shape, boundary conditions and material properties. Although there are exact analytical solutions for the buckling load of rectangular plates under certain boundary and loading conditions, thus far there are none for skew plates. Therefore numerical methods must be used for solution.

Thangam Babu and Reddy (1978) studied the stability analysis based on the Finite Strip Method for skew orthotropic plates subjected to in plane loadings. Edwardes and Kabaila (1978) investigated the buckling behaviour of simply supported skew plates and proposed refinements to the finite element displacement method. Chelladurai *et al.* (1984) developed a triangular orthotropic finite element to study the stability aspects of orthotropic as a function of fibre orientation under arbitrary loading. Shi (1990) presented a numerical solution technique by the boundary element method for the flexural vibration and buckling analysis of elastic orthotropic plates. Wang *et al.* (1992) studied the elastic buckling of skew plates subjected to in-plane loading by using Rayleigh-Ritz method with proposed pb-2 Ritz functions which consist of the product of a two dimensional polynomial function and a basic function. Civalek (2004) compared the methods of differential quadrature and harmonic differential quadrature and carried out

* Corresponding author, Mr., E-mail: darilmazk@itu.edu.tr

buckling, bending and free vibration analysis of thin isotropic plates and columns. Zhong and Gu (2006) concerned with the buckling analysis of simply supported rectangular Reissner-Mindlin plates subjected to linearly varying edge loads, Wang *et al*. (2007, 2008) studied the buckling of thin rectangular plates with non-linearly distributed compressive loading on two opposite sides by using differential quadrature method. Dhananjaya *et al*. (2009) presented a new 8-node serendipity quadrilateral plate bending element based on Mindlin-Reissner theory for the analysis of thin to moderately thick plate bending problems using Integrated Force Method. Gurses *et al*. (2009) studied the free vibration analysis of symmetric laminated skew plates by discrete singular convolution technique based on first-order shear deformation theory. Lee and Park (2009) performed a free vibration analysis of skew composite laminates with or without cutout based on the high-order finite element method. Civalek *et al*. (2010) presented buckling analysis of rectangular plates subjected to various in-plane compressive loads using Kirchhoff plate theory by adopting discrete singular convolution method.

The objective of the present work is to study the influence of aspect ratio and fýbre orientatýon on the stability of orthotropic skew plates. A four node assumed stress hybrid finite element previously proposed by the author is extended to include orthotropic material properties and used in this study.

2. Element formulation

Since Pian (1964) first established the assumed stress finite element model and derived the corresponding element stiffness matrix, the hybrid stress model has been shown highly accurate, and easy to fulfill the compatibility condition of the finite element method. The element developed in this paper is based on Hellinger-Reissner variational principle. The Hellinger-Reissner functional can be written as

$$\Pi_{RH} = \int_V \{\sigma\}^T [D]\{u\} dV - \int_V \frac{1}{2}\{\sigma\}^T [S]\{\sigma\} dV \tag{1}$$

where $\{\sigma\}$ is the stress vector, [S] is the material flexibility matrix relating strains, $\{\varepsilon\}$, to stress ($\{\varepsilon\} = [S]\{\sigma\}$), [D] is the differential operator matrix corresponding to the linear strain-displacement relations ($\{\varepsilon\} = [D]\{u\}$) and V is the volume of structure.

The approximation for stress and displacements can now be incorporated in the functional. The stress field is described in the interior of the element as

$$\{\sigma\} = [P]\{\beta\} \tag{2}$$

and a compatible displacement field is described by

$$\{u\} = [N]\{q\} \tag{3}$$

where [P] and [N] are matrices of stress and displacement interpolation functions, respectively, and $\{\beta\}$ and $\{q\}$ are the unknown stress and nodal displacement parameters, respectively. Intra-element equilibrating stresses and compatible (boundary or intra-element) displacements are independently interpolated. Since stresses are independent from element to element, the stress parameters are eliminated at the element level and a conventional stiffness matrix results. This leaves only the nodal displacement parameters to be assembled into the global system of equations. Therefore, use of hybrid-

stress versus assumed-displacement elements can be made transparent to general-purpose program users. Substituting the stress and displacement approximations Eq. (2), Eq. (3) in the functional Eq. (1).

$$\Pi_{RH} = [\beta]^T[G][q] - \frac{1}{2}[\beta]^T[H][\beta] \tag{4}$$

where

$$[H] = \int_V [P]^T[S][P]dV \tag{5}$$

$$[G] = \int [P]^T([D][N])dV \tag{6}$$

The elements of any row of the matrix [G] are the forces at the nodes when the stress in the element is represented by one column of [P]. The elements in any row of [G] represent a set of self-equilibrating forces.

The form of Eq. (5) and Eq. (6) is directly amenable to numerical integration. In principle, integration rules should be chosen which integrate all terms in [H] and [G] exactly. Arbitrary reduction of the integration order in [H] can lead to poor conditioning or singularity in [H] so that $[H]^{-1}$ will not exist, and reduction in [G] can lead to spurious zero energy modes since [G] controls element stiffness rank.

Now imposing stationary conditions on the functional with respect to the stress parameters $\{\beta\}$ gives

$$[\beta] = [H]^{-1}[G][q] \tag{7}$$

Substitution of $\{\beta\}$ in Eq. (4), the functional reduces to

$$\Pi_{RH} = \frac{1}{2}[q]^T[G]^T[H]^{-1}[G][q] = \frac{1}{2}[q]^T[K][q] \tag{8}$$

where

$$[K] = [G]^T[H]^{-1}[G] \tag{9}$$

is recognized as a stiffness matrix.

The solution of the system yields the unknown nodal displacements $\{q\}$. After $\{q\}$ is determined, element stresses or internal forces can be recovered by use of Eq. (7) and Eq. (2). Thus

$$\{\sigma\} = [P][H]^{-1}[G]\{q\} \tag{10}$$

In modelling structures using displacement based or hybrid elements, body forces applied to the elements are replaced by equivalent nodal forces. With this replacement, the stiffness and stress matrices in element formulations need only to be considered for forces applied at the nodes.

The stress stiffness matrix is derived by using the Green-Lagrange strains which correspond to defining the strain of a line segment by the equation

$$\varepsilon = \frac{1}{2}\left[\left(\frac{ds^*}{ds}\right)^2 - 1\right] \tag{11}$$

where ds and ds* are respectively the initial and final lengths of the line segment.
The nonlinear terms are retained only for the membrane strains. The membrane strains are written as

$$\{\varepsilon\} = \varepsilon_L + \{\varepsilon_{NL}\} \tag{12}$$

where the linear part is given by

$$\{\varepsilon_L\} = \begin{Bmatrix} \varepsilon_{xL} \\ \varepsilon_{yL} \\ \gamma_{xyL} \end{Bmatrix} = \begin{Bmatrix} u,_x \\ v,_y \\ u,_y + v,_x \end{Bmatrix} \tag{13}$$

and the nonlinear part is given by

$$\{\varepsilon_{NL}\} = \begin{Bmatrix} \varepsilon_{xNL} \\ \varepsilon_{yNL} \\ \gamma_{xyNL} \end{Bmatrix} = \begin{Bmatrix} \frac{1}{2}(u,_x^2 + v,_x^2 + w,_x^2) \\ \frac{1}{2}(u,_y^2 + v,_y^2 + w,_y^2) \\ u,_x u,_y + v,_x v,_y + w,_x w,_y \end{Bmatrix} \tag{14}$$

The bending strains are computed using the changes in curvature by

$$\{\chi\} = \begin{Bmatrix} \chi_x \\ \chi_y \\ \chi_{xy} \end{Bmatrix} = \begin{Bmatrix} \theta_{y,x} \\ -\theta_{x,y} \\ \theta_{y,y} - \theta_{x,x} \end{Bmatrix} \tag{15}$$

The transverse shear strains are given by

$$\{\gamma\} = \begin{Bmatrix} \gamma_{xz} \\ \gamma_{yz} \end{Bmatrix} = \begin{Bmatrix} \theta_y + w,_x \\ -\theta_x + w,_y \end{Bmatrix} \tag{16}$$

The generalized Hellinger-Reissner functional including the nonlinear strains can be written as

$$\Pi_{RH} = \int_V \{\sigma\}^T [D]\{u\} dV - \frac{1}{2}\int_V \{\sigma\}^T [S]\{\sigma\} dV + \int_V \{\sigma_o\}^T \{\varepsilon_{NL}\} dV \tag{17}$$

where $\{\sigma_o\}$is the prescribed prebuckling stress state. Substituting the stress and displacement approximations Eq. (5), Eq. (6) in the functional

$$\Pi_{RH} = [\beta]^T [G][q] - \frac{1}{2}[\beta]^T [H][\beta] + \frac{1}{2}\{q\}^T [K_\sigma]\{q\} \tag{18}$$

and stress stiffness matrix is given by

$$[K_\sigma] = \int_A [N]^T [N']^T [\psi][N'][N] dA \tag{19}$$

respectively.

Here $[N']$ is obtained from shape functions [N] by appropriate differentiation and ordering of terms.

$$[N'] = \begin{bmatrix} \partial/\partial x & 0 & 0 & 0\ 0\ 0 \\ \partial/\partial y & 0 & 0 & 0\ 0\ 0 \\ 0 & \partial/\partial x & 0 & 0\ 0\ 0 \\ 0 & \partial/\partial y & 0 & 0\ 0\ 0 \\ 0 & 0 & \partial/\partial x & 0\ 0\ 0 \\ 0 & 0 & \partial/\partial y & 0\ 0\ 0 \end{bmatrix} \tag{20}$$

The matrix $[\psi]$, which corresponds to the pre-buckling stress state, consists of membrane stress resultants which are evaluated from a linear static stress analysis. It is given by

$$[\psi] = \begin{bmatrix} \mu & 0 & 0 \\ 0 & \mu & 0 \\ 0 & 0 & \mu \end{bmatrix} \tag{21}$$

where

$$[\mu] = \begin{bmatrix} N_x & N_{xy} \\ N_{xy} & N_y \end{bmatrix} \tag{22}$$

3. Governing Equations

Consider a plate of uniform thickness which the orthotropic material property may be arbitrarily oriented at an angle ϕ with reference to the x-axis of the local coordinate system Fig. 1

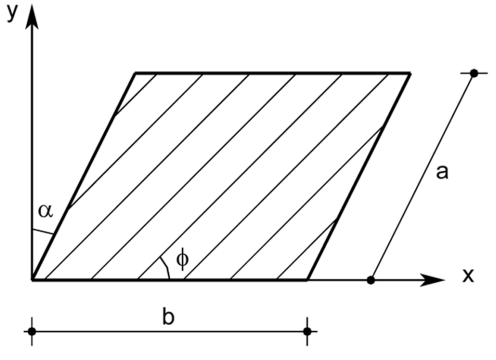

Fig. 1 Sketch of plate geometry

The stress-strain relation with respect to x, y and z axes can be written as

$$\begin{Bmatrix}\sigma_x\\ \sigma_y\\ \tau_{xy}\end{Bmatrix}=\begin{bmatrix}\bar{D}_{11} & \bar{D}_{12} & \bar{D}_{16}\\ \bar{D}_{12} & \bar{D}_{22} & \bar{D}_{26}\\ \bar{D}_{16} & \bar{D}_{26} & \bar{D}_{66}\end{bmatrix}\begin{Bmatrix}\varepsilon_x\\ \varepsilon_x\\ \gamma_{xy}\end{Bmatrix} \quad \text{or} \quad \{\sigma\}=[\bar{D}_{ij}]\{\varepsilon\} \qquad (i,j=1,2,3) \tag{23}$$

$$\begin{Bmatrix}\tau_{xz}\\ \tau_{yz}\end{Bmatrix}=\begin{bmatrix}\bar{D}_{44} & \bar{D}_{45}\\ \bar{D}_{45} & \bar{D}_{55}\end{bmatrix}\begin{Bmatrix}\gamma_{xz}\\ \gamma_{yz}\end{Bmatrix} \quad or \quad \{\tau\}=[\bar{D}_{ij}]\{\gamma\} \qquad (i,j=4,5) \tag{24}$$

The elasticity tensor $[\bar{D}_{ij}]$ in Eqs. (23) and (24) is defined as

$$[\bar{D}_{ij}]=[T_1]^{-1}[D_{ij}][T_1]^{-T} \quad (i,j=1,2,6) \tag{25}$$

$$[\bar{D}_{ij}]=[T_2]^{-1}[D_{ij}][T_2] \quad (i,j=4,5) \tag{26}$$

in which

$$[T_1]=\begin{bmatrix}\cos^2\phi & \sin^2\phi & 2\sin\phi\cos\phi\\ \sin^2\phi & \cos^2\phi & -2\sin\phi\cos\phi\\ -\sin\phi\cos\phi & \sin\phi\cos\phi & \cos^2\phi-\sin^2\phi\end{bmatrix} \tag{27}$$

$$[T_2]=\begin{bmatrix}\cos\phi & -\sin\phi\\ \sin\phi & \cos\phi\end{bmatrix} \tag{28}$$

Here [T1] and [T2] are the tranformation matrices between the axes of orthotropy and the reference axes x-y .

$$[D_{ij}]=\begin{bmatrix}D_{11} & D_{12} & 0\\ D_{12} & D_{22} & 0\\ 0 & 0 & D_{66}\end{bmatrix} \quad (i,j=1,2,6) \quad ,[D_{ij}]=\begin{bmatrix}D_{44} & 0\\ 0 & D_{55}\end{bmatrix} \qquad (i,j=4,5) \tag{29}$$

$$D_{11}=\frac{E_1}{1-\nu_{12}\nu_{21}} \qquad D_{12}=\frac{\nu_{12}E_2}{1-\nu_{12}\nu_{21}} \qquad D_{22}=\frac{E_2}{1-\nu_{12}\nu_{21}} \tag{30}$$

$$D_{66}=G_{12} \qquad D_{44}=G_{13} \qquad D_{55}=G_{23} \tag{31}$$

The stress resultants are given by

$$\begin{bmatrix} M_x \\ M_y \\ M_{xy} \end{bmatrix} = \int_{-h/2}^{h/2} \begin{bmatrix} \sigma_x \\ \sigma_y \\ \tau_{xy} \end{bmatrix} \cdot z\,dz \tag{32}$$

$$\begin{bmatrix} Q_x \\ Q_y \end{bmatrix} = \int_{-h/2}^{h/2} \begin{bmatrix} \tau_{xz} \\ \tau_{yz} \end{bmatrix} dz \tag{33}$$

From Eqs (32). and (33) the constitutive equations of the plate are obtained as

$$\{F\} = [E]\{\chi\} \tag{34}$$

where

$$\{F\} = \{M_x, M_y, M_{xy}, Q_x, Q_y\} \tag{35}$$

$$\{\chi\} = \{\kappa_x, \kappa_y, \kappa_{xy}, \gamma_{xz}, \gamma_{yz}\} \tag{36}$$

The elasticity matrix can be expressed as

$$[E] = \begin{bmatrix} [A_{ij}] & 0 \\ 0 & [B_{ij}] \end{bmatrix} \tag{37}$$

in which

$$[A_{ij}] = \int_{-h/2}^{h/2} [\bar{D}_{ij}] z^2 dz \qquad (i, j=1, 2, 6) \tag{38}$$

$$[B_{ij}] = \int_{-h/2}^{h/2} [\bar{D}_{ij}] dz \qquad (i, j=4, 5) \tag{38}$$

4. The hybrid stress element

The proposed element is generated by a combination of a hybrid membrane element and a hybrid plate element.

4.1. Membrane component of the element with drilling degree of freedom

Generally membrane elements have two translational d.o.f (u,v) per node but the need for membrane elements with a drilling degree of freedom arises in many engineering problems. A drilling rotation is defined as inplane rotation about the axis normal to the plane of element. This type of element provides

an easy coupling with edge beams which have six d.o.f per node. Inclusion of a drilling degree of freedom gives also the improved behavior of the element (Allman 1984, Choi and Lee 1996). The possibility of membrane elements with drilling d.o.f was opened by Allman (1984), Bergan and Felippa (1985). The concept has been further elaborated by many other researchers (Cook 1986, MacNeal and Harder 1988, Yunus et. al. 1989, Ibrahimbegovic et. al. 1990, Choi and Lee 1996, Darilmaz 2007, 2009) for more improved elements.

Formulation of drilling d.o.f for the present element is based on the procedure given by Yunus et. al. (1989). The displacement fields are expressed in terms of translational and rotational d.o.f.'s at the corner nodes only.

The membrane displacement field for the 4-node element is derived from an 8-node element, Fig. 2.

Rotational d.o.f. are associated with parabolic displaced shapes of element sides. In Fig. 3, rotational d.o.f. θ_{zi} and θ_{zj} are shown at nodes i and j of the element side of length L.

δ can be regarded as quadratic in side-tangent coordinates. θ_{zi} and θ_{zj} produce the edge normal displacement δ and midside value δ_m

$$\delta = \frac{s(L-s)}{2L}(\theta_{zi} - \theta_{zj}) \qquad \delta_m = \frac{L}{8}(\theta_{zi} - \theta_{zj}) \tag{40}$$

The x and y components of δ are $\delta \cos\alpha$ and $\delta \sin\alpha$. Therefore, after adding the contribution to displacement from nodes i and j, the total displacements u and v of a typical point on the edge are

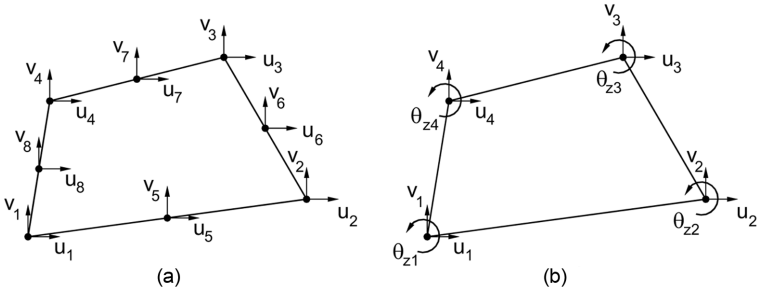

Fig. 2 Displacements for (a) 8-node membrane (b) 4-node membrane

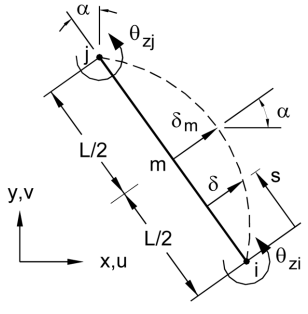

Fig. 3 Side displacement produced by drilling degrees of freedoms θ_{zi} and θ_{zj}

$$\begin{Bmatrix} u \\ v \end{Bmatrix} = \frac{L-s}{L}\begin{Bmatrix} u_i \\ v_i \end{Bmatrix} + \frac{s}{L}\begin{Bmatrix} u_j \\ v_j \end{Bmatrix} + \frac{(L-s)s}{2L}(\theta_{zj} - \theta_{zi})\begin{Bmatrix} \cos\alpha \\ \sin\alpha \end{Bmatrix} \tag{41}$$

Side 1-5-2 of the element, Fig. 2 d.o.f. at node 5 are related to d.o.f. at nodes 1 and 2 of the element. By evaluating Eq. 2 with $s = L / 2$ with $i = 1$, $j = 2$, $L\cos\alpha = y_2 - y_1$ and $L\sin\alpha = x_1 - x_2$, yields

$$\begin{Bmatrix} u_5 \\ v_5 \end{Bmatrix} = \frac{1}{2}\begin{Bmatrix} u_1 \\ v_1 \end{Bmatrix} + \frac{1}{2}\begin{Bmatrix} u_2 \\ v_2 \end{Bmatrix} + \frac{(\theta_{zj} - \theta_{zi})}{8}\begin{pmatrix} y_2 - y_1 \\ x_1 - x_2 \end{pmatrix} \tag{42}$$

Aafter doing the same for d.o.f. at nodes 6, 7 and 8 d.o.f. in Fig.1 (b) and (c) by the transformation, the complete relation can be written

$$\{u_1\ v_1\ u_2\ v_2\ \ldots\ u_8\ v_8\}^T = [T]_{16\times 12}\{q\}^T_{membrane} \tag{43}$$

Where

$$\{q\}_{membranae} = \{u_1\ v_1\ \theta_{z1}\ u_2\ v_2\ \theta_{z2}\ u_3\ v_3\ \theta_{z3}\ u_4\ v_4\ \theta_{z4}\} \tag{44}$$

So the midside nodal displacements can be written in terms of the corner nodal displacements and rotations and the displacement field for the 4-node, twelve d.o.f. membrane element can be derived from an 8-node membrane element. This is done through the use of the transformation matrix [T].

The assumed stress field for the membrane part which satisfies the equilibrium conditions for zero body forces and avoid rank deficiency is given as

$$\begin{aligned} N_x &= \beta_1 + \beta_2 x + \beta_3 y + \beta_4 x^2 + \beta_5 xy + \beta_6 y^2 \\ N_y &= \beta_4 y^2 + \beta_7 + \beta_8 x + \beta_9 y + \beta_{10} x^2 + \beta_{11} xy \\ N_{xy} &= -\beta_2 y - 2\beta_4 xy - \beta_5 y^2/2 - \beta_9 x - \beta_{11} x^2/2 + \beta_{12} \end{aligned} \tag{45}$$

4.2. Plate component of the element

The flexural component of the element is identical to that of the plate bending element presented by the author, Darllmaz (2005 and 2007), and corresponds to the Mindlin/Reissner plate theory. For the Mindlin plates, only C^0 continuity is required, and therefore the difficulties of C^1 continuity requirement for thin plate element are solved easily. Moreover, both thin and thick plate analyses can be integrated into one element model.

The biggest difficulty in deriving hybrid finite elements seems to be the lack of a rational methodology for deriving stress terms. It is recognized that the number of stress modes m in the assumed stress field should satisfy

$$m \geq n - r \tag{46}$$

With n the total number of nodal displacements, and r the number of rigid body modes in an element. If

Eq. is not satisfied, use of too few coefficients in {β}, the rank of the element stiffness matrix will be less than the total degrees of deformation freedom and the numerical solution of the finite element model will not be stable and produces on element with one or more mechanism.

Increasing the number of β's by adding stress modes of higher-order term, each extra term will add more stiffness and stiffens the element.

The element has 12 d.o.f, three of which are associated with the out of plane rigid body motions. Therefore, a stress field with a minimum of 9 independent parameters is needed to describe the stress field.

The assumed stress field which satisfies the equilibrium conditions for zero body forces and avoids rank deficiency for the plate part is given as

$$\begin{aligned} M_x &= \beta_1 + \beta_4 y + \beta_6 x + \beta_8 xy \\ M_y &= \beta_2 + \beta_5 x + \beta_7 y + \beta_9 xy \\ M_{xy} &= \beta_3 + \beta_{10} x + \beta_{11} y + \beta_{12} x^2/2 + \beta_{13} y^2/2 \\ Q_x &= \beta_6 + \beta_{11} + \beta_8 y + \beta_{13} y \\ Q_y &= \beta_7 + \beta_{10} + \beta_9 y + \beta_{12} y \end{aligned} \tag{47}$$

Numerical experimentations indicate that this 13 parameter selection of stress field is somewhat more accurate and less sensitive to geometric distortion than fewer parameter selections. This selection of stresses produces no spurious zero energy modes. It is observed stress field remains invariant upon node numbering, Darllmaz (2005).

The nodal displacements for the plate are chosen as

$$\{q\}_{plate} = \{w_1\ \theta_{x1}\ \theta_{y1}\ w_2\ \theta_{x2}\ \theta_{y2}\ w_3\ \theta_{x3}\ \theta_{y3}\ w_4\ \theta_{x4}\ \theta_{y4}\} \tag{48}$$

The combination of membrane and plate element yields the element which has 6 d.o.f per node and totally 24 d.o.f .

While obtaining the stiffnes matrix a 4x4 point Gauss-Legendre scheme is chosen to avoid ill conditioning or singularity.

5. Numerical Examples

5.1. Buckling of an isotropic simply supported skew plate

The buckling load of a skew plate for assessing the accuracy of the element and the results obtained are compared with other solutions. Comparison of the values of k for an isotropic skew plate is given in Table 1.

The lowest theoretical buckling load of uniaxially loaded rectangular plate which is simply supported on all four edges and is of width a, length b and thickness t is $N_{cr} = k\pi^2 Et^3/12(1-v^2)b$ where $k = (a/b + b/a)^2$.

The results obtained for a / b = 1 ($\alpha = 0^o$ to 45^o) and a / b = 2 ($\alpha = 0^o$) values are presented in Table 1

Table 1 Nondimensional critical load parameter k for rectangular plate

a/b	Skew Angle	Present Study	Analytical	% Diff	Buckling Mode Shape
1	0	3.94	4.0	1.50	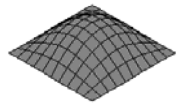
1	15	4.22	4.287	1.56	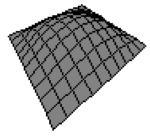
1	30	5.21	5.333	2.31	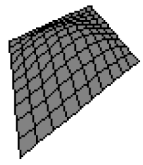
1	45	7.63	8.0	4.63	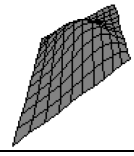
2	0	6.13	6.25	1.92	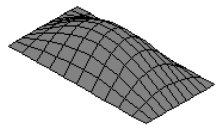

and results showed that the behaviour of the element is satisfactory, converges to the analytical values. The analytical solutions are extracted from Durvasula(1971).

5.2. Convergence of Element

For assessing the convergence of the element the buckling load parameter of a simply supported square plate is obtained for different meshes. Variation of k for different number of elements is given in Fig. 4. It can be seen that the solution converges to the theoretical solution.

5.3. Influence of aspect ratio and fibre orientation

Some numerical examples are used by using the above formulation to study the influence of aspect ratio, fibre orientation on the stability of simply supported skew plates. The values of the nondimensional critical load parameter k, ($k = 12\ N_{cr}b / \pi^2 D_{66} t^3$), are obtained for different aspect ratios (a/b), fibre orientations and two different loadings. The material properties are taken as $E_1 = 3.8 \times 10^7$ kN/m^2, $E_2 = 8.3 \times 10^6$ kN/m^2, $G_{12} = 4.1 \times 10^6$ kN/m^2, $\nu_{12} = 0.26$.

Variation of nondimensional critical load parameter k with aspect ratio for different fibre orientations is shown in Figs 5-13. Naming of graphs are based on P_α_ϕ notation. As an example P_45_30 indicates a plate with a skew angle 45^o and a fiber orientation 30^o.

The following observations can be made from these Figures. Individual or combined variation of

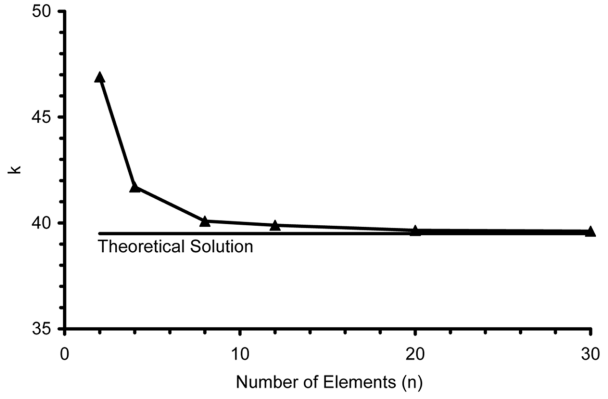

Fig. 4 Convergence of k with number of elements for a square isotropic plate

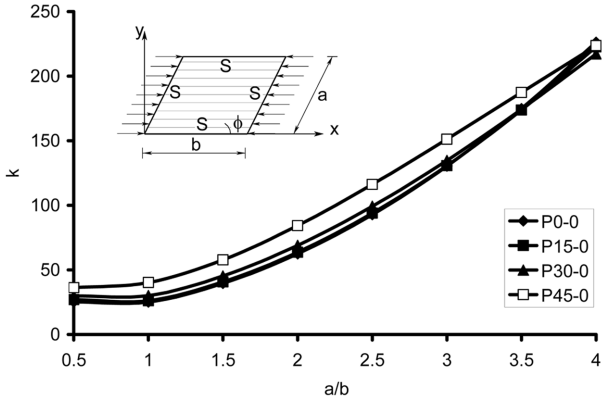

Fig. 5 Variation of k with aspect ratio for $\phi = 0^o$ (uniform inplane load)

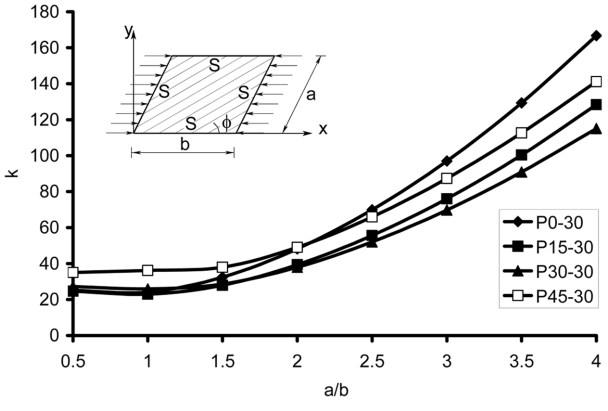

Fig. 6 Variation of k with aspect ratio for $\phi = 30^o$ (uniform inplane load)

skew angle, aspect ratio, fiber orientation is found to have great influence on the stability of plate. The values of buckling load parameter increase with the skew angle α. This is because the area of the plate

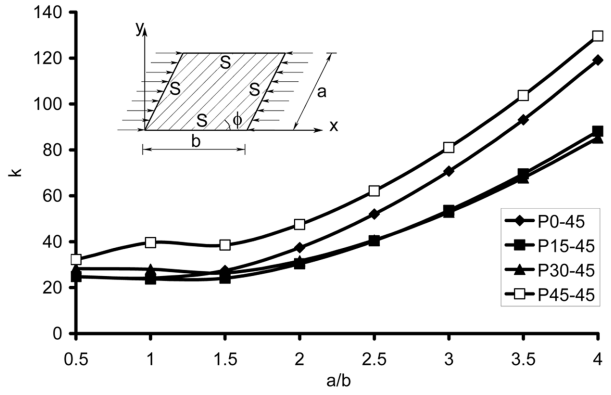

Fig. 7 Variation of k with aspect ratio for $\phi = 45^{o}$ (uniform inplane load)

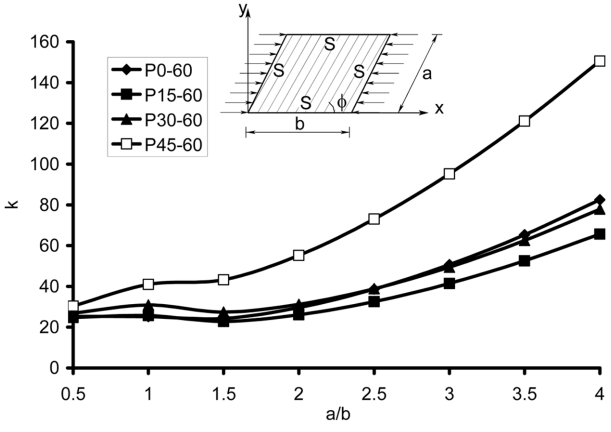

Fig. 8 Variation of k with aspect ratio for $\phi = 60^{o}$ (uniform inplane load)

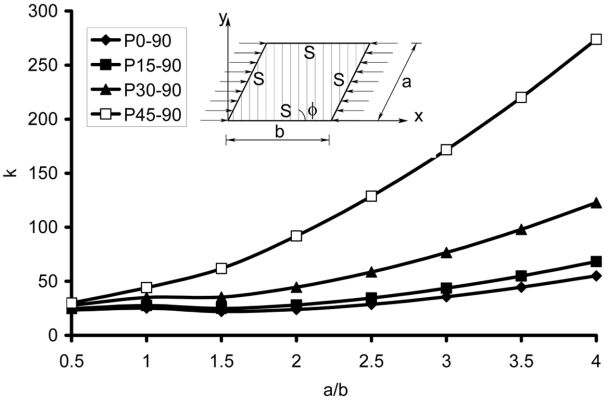

Fig. 9 Variation of k with aspect ratio for $\phi = 90^{o}$ (uniform inplane load)

and the perpendicular distance between the nonskew edges decrease as the skew angle increases. Due to the reduction in area, the stiffness of the plate increases, hence, the buckling load increases. The buckling

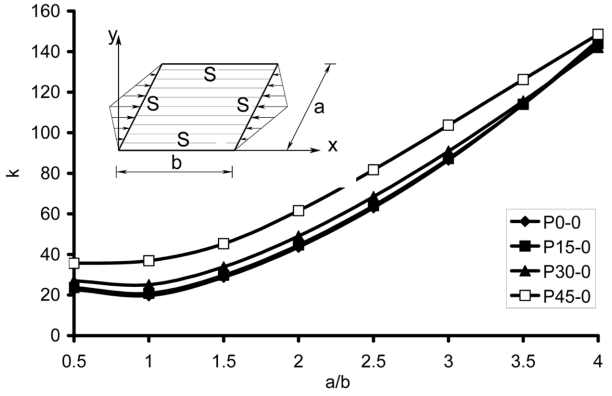

Fig. 10 Variation of k with aspect ratio for $\phi = 0^o$ (triangular inplane load)

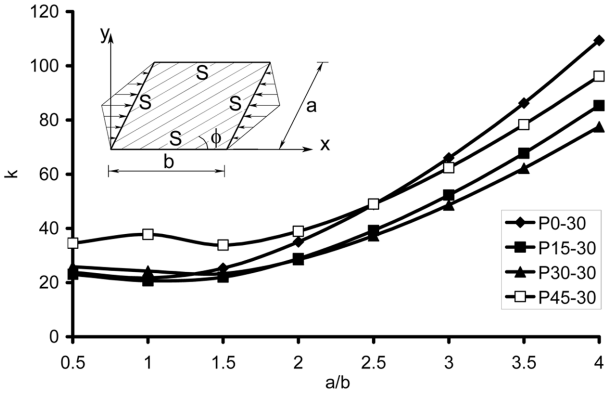

Fig. 11 Variation of k with aspect ratio for $\phi = 30^o$ (triangular inplane load)

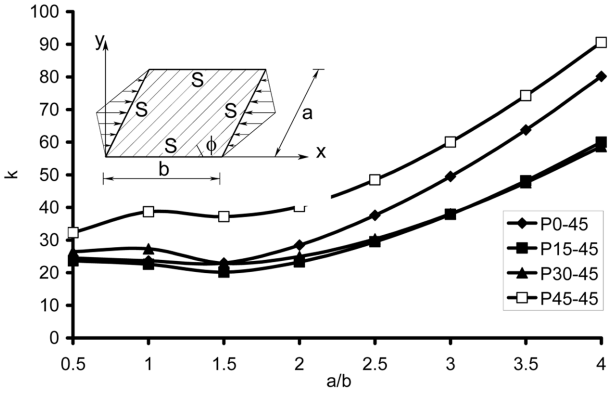

Fig. 12 Variation of k with aspect ratio for $\phi = 45^o$ (triangular inplane load)

load parameters obtained from uniform load solutions are greater than the triangular load solutions.

A 12 × 12 mesh is used for a/b = 1 and 48 × 12 mesh for a / b = 4 for all skew angles. Convergence is

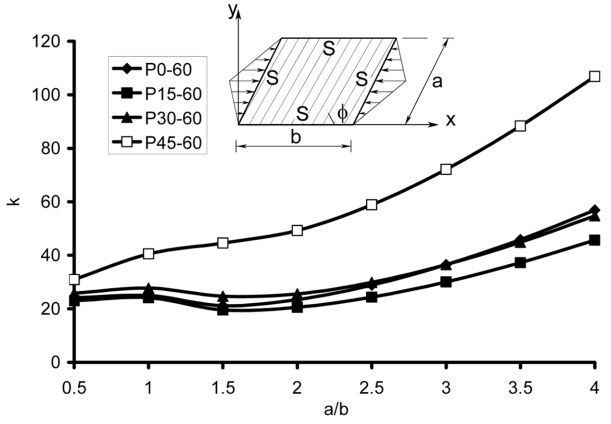

Fig. 13 Variation of k with aspect ratio for $\phi = 60^{o}$ (triangular inplane load)

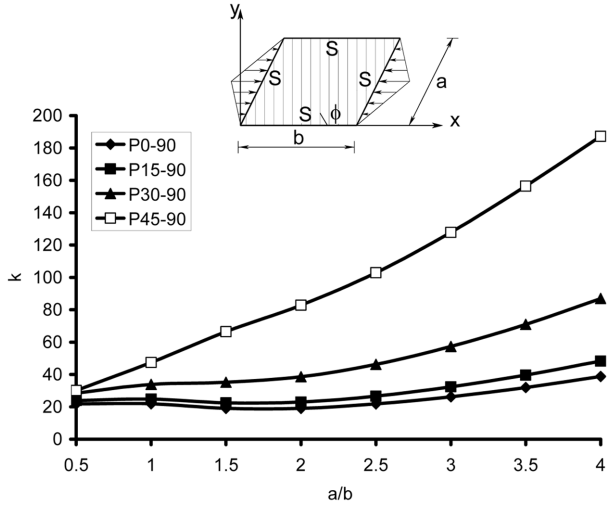

Fig. 14 Variation of k with aspect ratio for $\phi = 90^{o}$ (triangular inplane load)

investigated for refined meshes and found that skew angle has small effect on the convergence of buckling loads. The highest skew angle for this study is 45°.

6. Conclusions

The plate bending element which corresponds to the Mindlin/Reissner plate theory has been extended for the buckling analysis of simply supported orthotropic skew plates. The buckling load parameter k are determined for skew orthotropic plates under uniform and triangular compression in the x-direction.

The results obtained from this study may be summarised as the buckling load of simply supported skew plates is apparently influenced by aspect ratio, skew angle, fiber orientation and the loading shape. The buckling load parameter of plates increases while increasing aspect ratio (a/b), the skew angle (α) and the rigidity of the plate.

References

Allman, D. J., (1984), "A compatible triangular element including vertex rotations for plane elasticity problems", *Comp. Struct.*, **19**(1-2), 1-8.

Bergan, P. G. And Felippa, C. A. (1985), "A triangular membrane element with rotational degrees of freedom", *Comp. Methods Appl. Mech. Eng.*, **50**(1), 25-69.

Chelladurai T., Shastry B. P., Rao, G. V., (1984), "Effect of Fibre Orientation on the Stability of Orthotropic Rectangular Plates", *Fibre Science and Technology*, **20**(2), 121-134.

Choi, C. K., and Lee, W. H. (1996), "Versatile variable-node flat-shell element", *J. Eng. Mech*., **122**(5), 432–441.

Civalek O, Korkmaz A., Demir C., (2010), "Discrete singular convolution approach for buckling analysis of rectangular Kirchhoff plates subjected to compressive loads on two-opposite edges", *Adv. Eng. Softw.*, **41**(4), 557-560.

Civalek, Ö. (2004), "Application of Differential Quadrature (DQ) and Harmonic Differential Quadrature (HDQ) For Buckling Analysis of Thin Isotropic Plates and Elastic Columns", *Eng. Struct.,* **26**(2), 171-186.

Gürses, M., Civalek, Ö., Korkmaz, A. and Ersoy, H. (2009), "Free vibration analysis of symmetric laminated skew plates by discrete singular convolution technique based on first-order shear deformation theory", *Int. J. Numer. Meth. Eng.,* **79**(3), 290-313.

Cook, R. D., (1986), "On the Allman triangle and a related quadrilateral element", *Comp. Struct.*, **22**(6), 1065-1067.

Darilmaz, K. (2005), "An assumed-stress finite element for static and free vibration analysis of Reissner-Mindlin plates", *Struct. Eng. Mech.*, **19**(2), 199-215.

Darilmaz, K. (2007), "An assumed-stress hybrid element for static and free vibration analysis of folded plates", *Struct. Eng. Mech.*, **25**(4), 405-421.

Darilmaz, K. (2009), "An assumed-stress hybrid element for modeling of plates with shear deformations on elastic foundation", *Struct. Eng. Mech.*, **33**(5), 573-588.

Dhananjaya, H.R., Pandey, P.C. and Nagabhushanam, J. (2009), "New eight node serendipity quadrilateral plate bending element for thin and moderately thick plates using Integrated Force Method". *Struct. Eng. Mech.* **33**(4)485-502.

Durvasula, S. (1971) "Buckling of simply supported skew plates" *J. Engrg. Mech. Div., ASCE*, **97**(3), 967-979.

Edwardes, R. J., and Kabaila, A. P, (1978) "Buckling of simply supported skew plates", *Int. J. Numer. Methods Engrg.*, **12**(5), 779-785.

Ibrahimbegovic, A., Taylor, R. L. and Wison, E. L., (1990), "A robust quadrilateral membrane finite element with drilling degrees of freedom", *Int. J. Numer. Methods Eng.*, **30**(3), 445-457.

Lee, S.Y. and Park, T. (2009), "Free vibration of laminated composite skew plates with central cutouts". *Struct. Eng. Mech.* **31**(5)587-603.

MacNeal, R. H. And Harder, R. L., (1988), "A refined four-noded membrane element with rotational degrees of freedom", *Comp. Struct.*, **28**(1), 75-84.

Pian T. H. H., (1964), "Derivation of element stiffness matrices by assumed stress distributions", *AIAA J.*, **12**, 1333-1336.

Shi G., (1990),"Flexural Vibration and buckling analysis of orthotropic plates by the boundary element method", *Int. J. Solids Structures*, **26**(12), 1351-1370.

Thangam Babu P.V., Reddy D. V., (1978) "Stability analysis of skew orthotropic plates by the finite strip method", *Computers & Structures*, **8**(5), 599-607.

Wang, C. M. ; Liew, K.M.; Alwis, W.A.M. (1992), "Buckling of skew plates and corner condition for simply supported edges", *Journal Of Engineering Mechanics-ASCE*, **118**(4), 651-662.

Wang, X., Gan, L., Zhang, Y.(2008), "Differential quadrature analysis of the buckling of thin rectangular plates with cosine-distributed compressive loads on two opposite sides", *Adv. Eng. Softw.,* **39**(6), 497–504.

Wang, X.W., Wang, X.F. and Shi, X.D., (2007), "Accurate buckling loads of thin rectangular plates under parabolic edge compressions by the differential quadrature method", *Int. J. Mech. Sci.* **49**(4), 447–453

Yunus S. M., Saigal S., Cook R. D., (1989), "On improved hybrid finite elements with rotational degrees of freedom*", Int. J. Numer. Meth. Eng.*, **28**(4), 785-800.

Zhong H., Gu, C., (2006), "Buckling of Simply Supported Rectangular Reissner-Mindlin Plates Subjected to Linearly Varying In-Plane Loading", *J. Engrg. Mech.,* **132**(5), 578-581.